

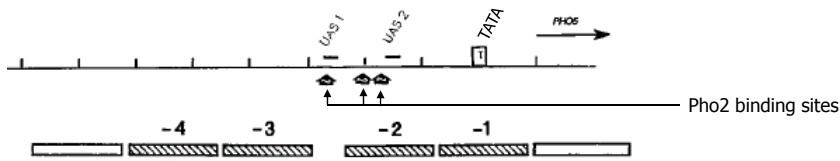
- Constitutively expressed genes ("housekeeping")
- Regulated genes (positive and negative feedbacks)
- Inducible genes ("on-off") and repressible genes ("off-on" ?)
- **Silenced genes (heterochromatic, CpG-methylated)**

Mechanistically, we say that inactive genes that can be reversibly activated are "poised" for activation, i.e. their status allows activation. Remember HCP-promoters from the genome-wide methylome study.

idem, of course, for histone modifications....

Caution:

we should avoid confusing the status of histone modifications at the "locus" (i.e. the part of chromosome where the gene sits), with the "local" histone status: if we concentrate to the very proximal part of promoters, often histone modifications are lost simply because histones are lost !



Pho4 is the P-sensitive inducer, whereas Pho2 is constitutive

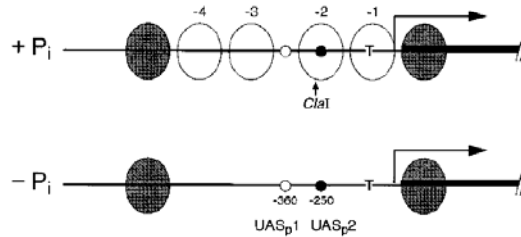


Figure 1. Chromatin Structure at the *PHO5* Promoter

Nucleosomes -1, -2, -3, and -4 are remodeled upon activation of the promoter by phosphate starvation conditions (Almer et al., 1986). The small circles mark UASp1 (open) and UASp2 (solid), which are Pho4-binding sites found by *in vitro* (Vogel et al., 1989) and *in vivo* (Venter et al., 1994) footprinting experiments. The positions are listed relative to the coding sequence (solid bar). T denotes the TATA box (Rudolph and Hinnen, 1987). The location of a *Cla*I site at -275 relative to the coding region is shown.

yeast

Chromatin remodeling is brought about by essentially these classes of factors:

1. **ATP-dependent chromatin remodelers.**
Enzymes that induce a topological change into nucleosomal DNA, altering DNA/histone interaction and/or the positioning of nucleosomes.
2. **HAT (histone acetyl transferases) (vs. HDAC histone deacetylases)**
Acetylation of the N-term of histones H3 & H4 reduces histone/DNA interaction and changes the conformation of nucleosomes in such a way that the nucleosomes are much less stable also translationally.
3. Histone demethylase (HDM) and methyltransferase (HMT)

Chromatin remodeling activities rely on quite large multiprotein **complexes** that are recruited to gene promoters by interaction with transcription factors

The nucleosomes positioned on *PHO5* promoter are "remodeled" after induction.

The prevailing model for understanding how a nucleosome can be "remodeled" foresees usual histone modifications, loosening of histone-DNA contacts, and **sliding away or removal** from that region, due to the activity of ATP-dependent Chromatin Remodeling Complexes (histone/nucleosome chaperons).

Histone modifications and mobilization follow very rapidly

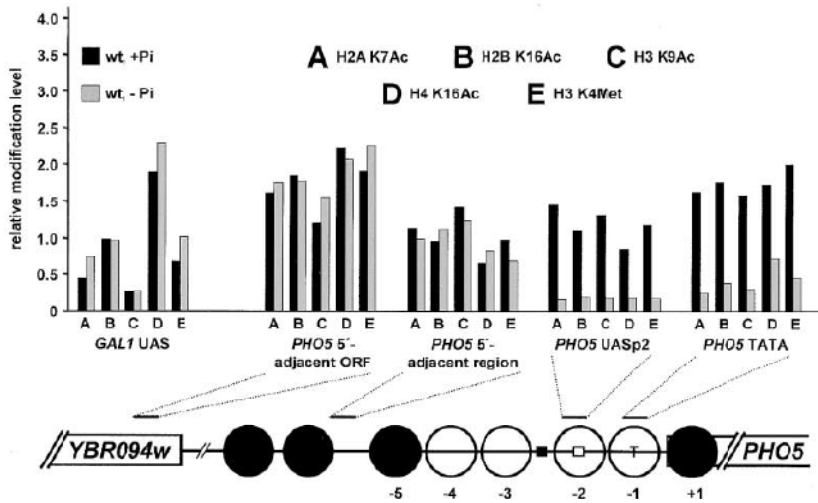
Molecular Cell, Vol. 11, 1599-1607, June, 2003, Copyright ©2003 by Cell Press

Histones Are First Hyperacetylated and Then Lose Contact with the Activated *PHO5* Promoter

Hans Reinke and Wolfram Hörz*
Adolf-Butenandt-Institut
Molekularbiologie
Universität München
Schillerstr. 44
D-80336 München
Germany

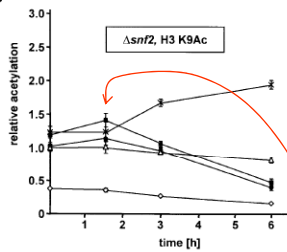
Summary

We have analyzed the histone modification status of the *PHO5* promoter from yeast by the ChIP technology and have focused on changes occurring upon activation. Using various acetylation-specific antibodies, we found a dramatic loss of the acetylation signal upon induction of the promoter. This turned out to be due, however, to the progressive loss of histones altogether. The fully remodeled promoter appears to be devoid of histones as judged by ChIP analyses. Local histone hyperacetylation does indeed occur, however, prior to remodeling. This can explain the delay in chromatin remodeling in the absence of histone acetyltransferase activity of the SAGA complex that was previously documented for the *PHO5* promoter. Our findings shed new light on the nucleosomal structure of fully remodeled chromatin. At the same time, they point out the need for novel controls when the ChIP technique is used to study histone modifications in the context of chromatin remodeling *in vivo*.



Using of a *snf2* defective strain: Snf2 is one of the major ATP-dependent chromatin remodelling enzymes in yeast.

B

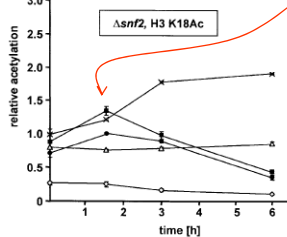


H3K9 acetylation / H3 occupancy			
time [h]	0	1.5	3
PHO5 5'-adjacent ORF	1.0	1.0	0.9
PHO5 UASp2	1.0	1.3	1.9
PHO5 TATA	1.0	1.1	1.7

Transient increase in H3K9 and H3K18 acetylation is now appreciated

Figure 4. Histone H3 hyper-acetylation at the Induced *PHO5* Promoter in a *snf2* Strain. Cells from strain 8141 (*snf2*) were induced by phosphate starvation, and the levels of histone H3 (A), H3 acetylated at lysine 9 (B), and at lysine 18 (C) were followed over time by ChIP. Acetylation levels normalized with respect to histone occupancy are listed in the tables. They were calculated by dividing the values for acetylated H3 by the H3 occupancy values. 0 time values were set to be 1.0.

C



H3K18 acetylation / H3 occupancy			
time [h]	0	1.5	3
PHO5 5'-adjacent ORF	1.0	0.9	1.0
PHO5 UASp2	1.0	1.7	2.4
PHO5 TATA	1.0	1.4	2.4

Other ATP-dep. Chromatin remodeling enzymes exist in yeast: removal of nucleosome is therefore **delayed**, but not abrogated.

These experiments say that we have

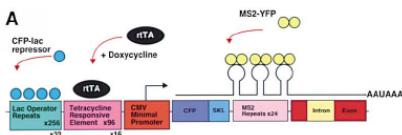
1. first, extensive histone acetylation, that reduces the strength of DNA/histone interaction
2. second (but immediate) the intervention of ATP-dep. chromatin remodeling complexes that displace nucleosome from the place

This is true o the PHO5 promoter in yeast, but ... does it represent the common mechanism ?

Cell, Vol. 116, 683–698, March 5, 2004, Copyright ©2004 by Cell Press

From Silencing to Gene Expression: Real-Time Analysis in Single Cells

Susan M. Janicki,¹ Toshiro Tsukamoto,²
Simone E. Salghetti,¹ William P. Tansey,¹
Ravi Sachidanandam,¹ Kannanganattu V. Prasanth,¹
Thomas Ried,³ Yaron Shav-Tal,⁴
Edouard Bertrand,⁵ Robert H. Singer,⁴
and David L. Spector^{1*}



Summary

We have developed an inducible system to visualize gene expression at the levels of DNA, RNA and protein in living cells. The system is composed of a 200 copy transgene array integrated into a euchromatic region of chromosome 1 in human U2OS cells. The condensed array is heterochromatic as it is associated with HP1, histone H3 methylated at lysine 9, and several histone methyltransferases. Upon transcriptional induction, HP1 α is depleted from the locus and the histone variant H3.3 is deposited suggesting that histone exchange is a mechanism through which heterochromatin is transformed into a transcriptionally active state. RNA levels at the transcription site increase immediately after the induction of transcription and the rate of synthesis slows over time. Using this system, we are able to correlate changes in chromatin structure with the progression of transcriptional activation allowing us to obtain a real-time integrative view of gene expression.

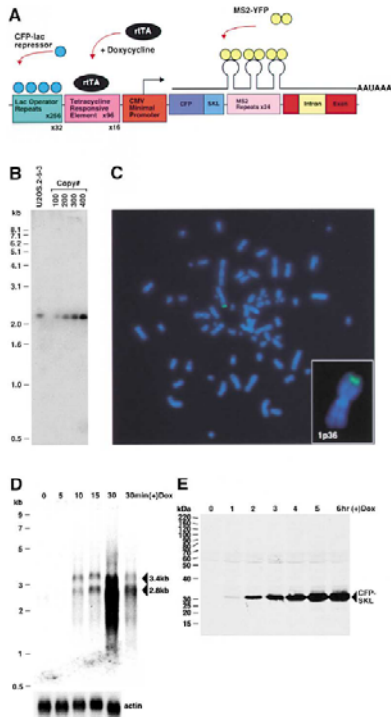
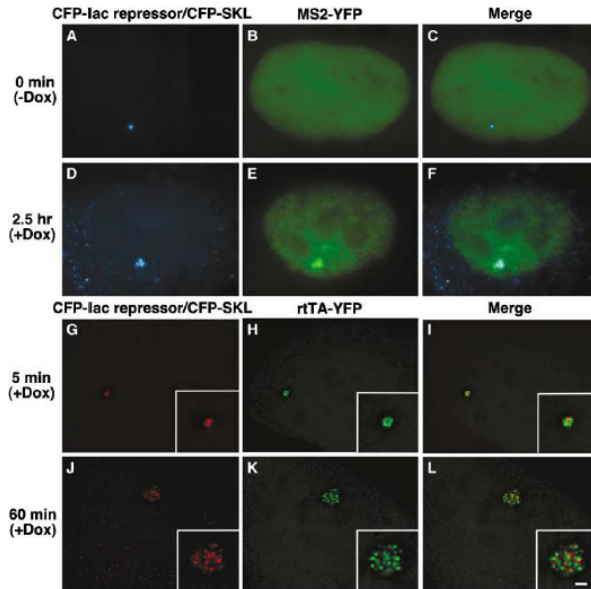


Figure 1. Characterization of Human U2OS 2-6-3 Cells

(A) Schematic representation of the gene expression plasmid, p3216PECMS2. The plasmid is composed of 256 copies of the lac operator, 9 tetracycline response elements, a minimal CMV promoter, CFP fused to the periclonal targeting signal SKL, 14 MS2 translational operators (MS2 repeats), a rabbit β -globin intron/exon module, and a cleavage/polyadenylation signal. Expression of CFP-lac repressor allows the DNA to be visualized and expression of pTet-On (rtTA) in the presence of doxycycline (dox) drives expression from the CMV minimal promoter. When MS2-YFP (YFP fused to the MS2 coat protein) dimerizes and interacts with the stem loop structure of the translational operator, it allows the transcribed RNA to be visualized. (B) Quantitative Southern blot of clone 2-6-3 genomic DNA. A 2.4 kb fragment is produced when clone 2-6-3 genomic DNA and p3216PECMS2 are digested with *Nco*I which cuts at the 5' end of CFP and within the β -globin intron. Comparison of known quantities of plasmid DNA equal to 100, 200, 300, and 400 copies per cell showed that 2-6-3 cells contain ~200 stably integrated copies of p3216PECMS2. (C) DNA fluorescence in situ hybridization (DNA FISH) of 2-6-3 cells shows that there is a single integration site in the euchromatic region of chromosome 1p36. (D) Northern blot time-course analysis of RNA isolated 0, 5, 10, 15, and 30 min after the induction of transcription. The last lane shows a lighter exposure of the 30 min time point. Pre-mRNA transcripts run at 3.4 kb and spliced mRNA at 2.8 kb. The probe recognizes the MS2 repeats. Actin was probed as a loading control. (E) Immunoblot time course analysis of CFP-SKL expression 0, 1, 2, 3, 4, 5, and 6 hr after the addition of doxycycline.



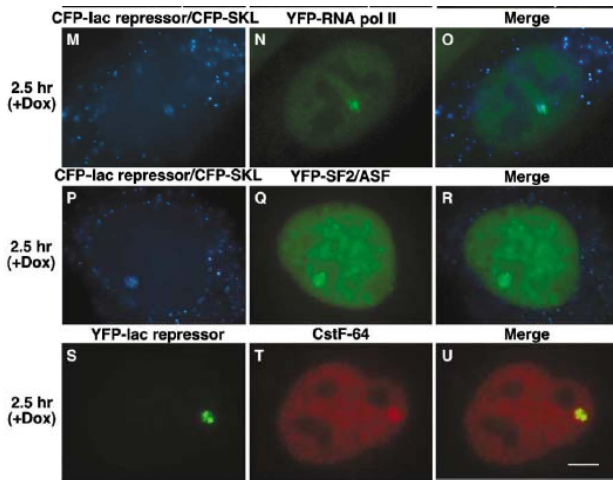


Figure 2. Visualization of DNA, RNA, and Protein in Living Cells

(A-F) U2OS 2-6-3 cells were transiently transfected with pSV2-CFP-lac repressor, pTet-ON (rtTA) and MS2-YFP, and imaging was begun 2.5 hr posttransfection.

(A-C) At 0 min (-) dox, CFP-lac repressor marks the locus (A) and MS2-YFP is diffusely distributed throughout the nucleus (B).

(D-F) 2.5 hr after the addition of Dox, the locus is highly decondensed and CFP-SKL is seen in the cytoplasmic peroxisomes (D). MS2-YFP accumulates at the site of the decondensed locus and is present in a particulate pattern throughout the nucleoplasm (E).

(G-L) Image stacks of cells expressing pSV2-CFP-lac repressor (pseudocolored red) and EYFP-rtTA-N1 (pseudocolored green) were collected and deconvolved in cells fixed 5 min (G-I) and 60 min (J-L) after the induction of transcription. Single sections from deconvolved stacks are shown.

(M-U) Factors involved in gene expression colocalize with the decondensed locus. YFP-RNA polymerase II (M-O), YFP-SF2/ASF (P-R), and Cstf64 (S-U) are present at the active locus. Scale bar is equal to 5 μ m. Scale bar in enlarged insets is equal to 1 μ m.

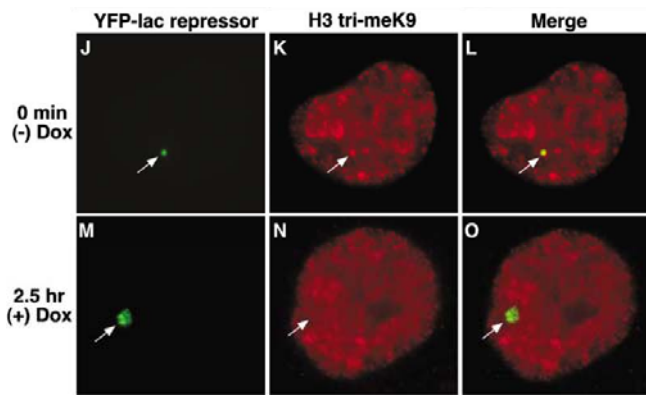
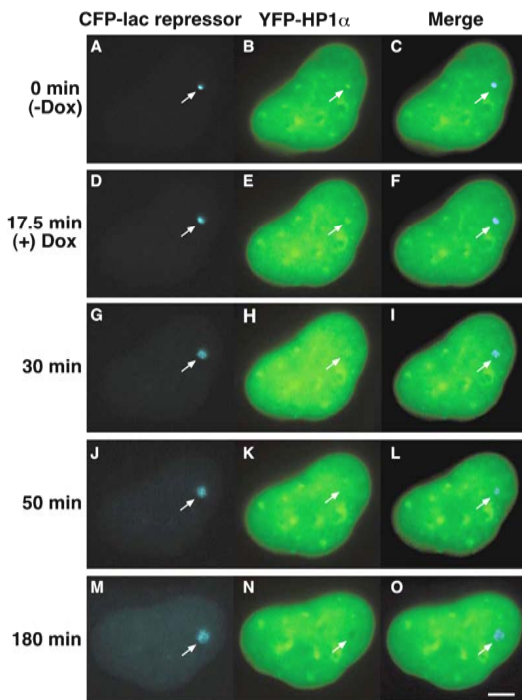
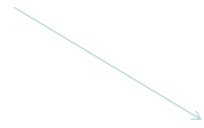


Figure 4. Characterization of the Condensed Heterochromatic Locus
YFP-HP1 (A-C), YFP-HP1 (D-F), and YFHP1 (G-I) colocalize with the condensed locus, marked by CFP-lac repressor and the histone H3 is trimethylated on lysine 9 (H3 trimeK9) (J-L). The H3 lysine 9 modification is not detected after the induction of transcription (M-O; 2.5 hr postdox).



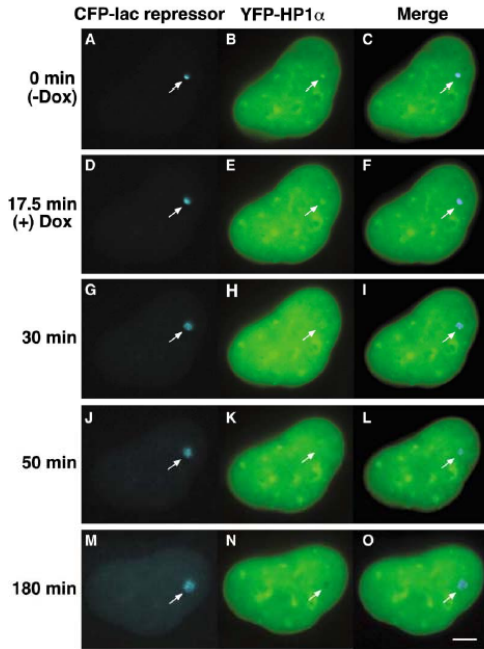


Figure 6. Dynamics of YFP-HP1 α Depletion from the Locus during Transcriptional Activation

YFP-HP1 α colocalizes with the condensed locus (0 min, A-C) and the condensed regions during the early time points of transcriptional activation (D-F, 17.5 min). It is seen in punctate structures at the 30 min time point (G-I) and appears smooth and diffuse by 50 min (J-L). 180 min postinduction, a dark region (HP1 α depleted) that colocalizes with the decondensed locus, is seen in the YFP-HP1 α image. Also see Supplemental Data and Supplemental Movie S2 available on Cell website. Scale bar is equal to 5 μ m.

Histone-modifying enzymes

Vedere Lezione "chromatin"

Histone Acetyltransferases HAT	-	Histone deacetylases HDAC
Histone Methyl transferases HMT	-	Histone demethylases

Several families – common domains – often domains that recognize other histone modifications. Often specific. They commonly make part of large multiprotein complexes and show a number of reciprocal interactions.

ATP-dependent chromatin remodeling complexes

Several types, with some context specificity. Sometimes very large multiprotein complexes.

Activity: "remodeling" of nucleosomes on a tract of DNA; removal of nucleosomes from DNA; reordering of nucleosomes on DNA; deposition of nucleosomes on new DNA (replication); isoform exchange.

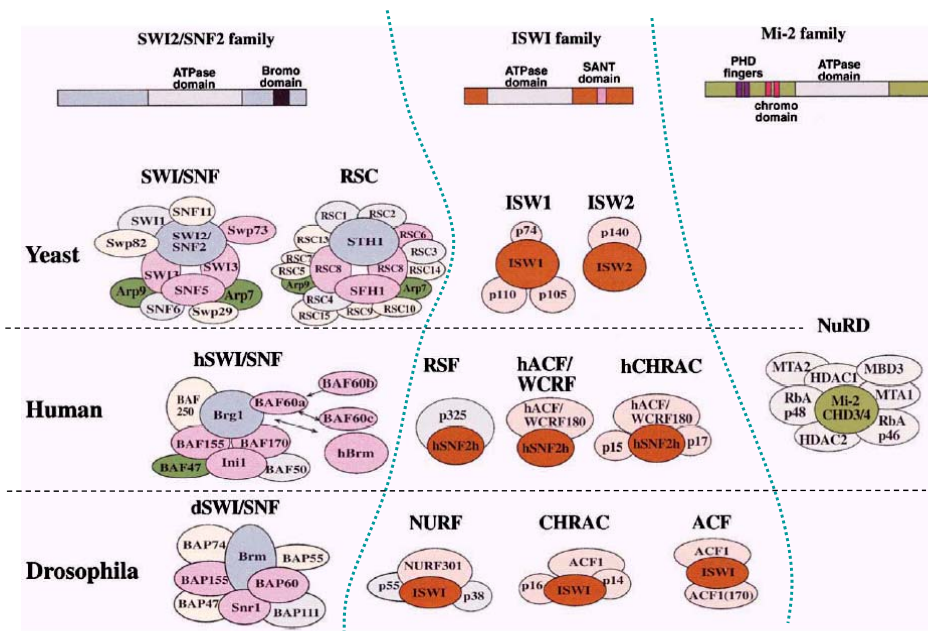


Figure 1. ATP-Dependent Remodeling Complexes

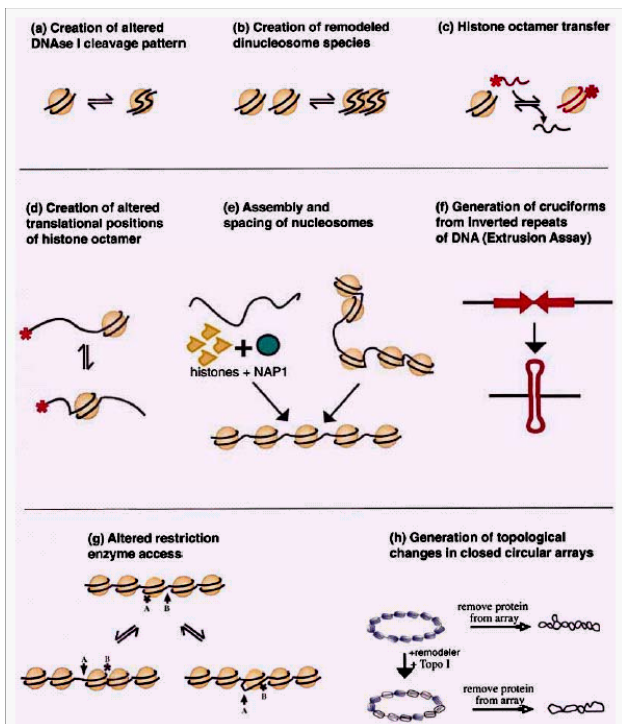


Figure 2. Biochemical Activities of ATP-dependent Remodeling Complexes
Each panel depicts a known activity of at least one remodeling complex (see text).

(a) The 10 bp pattern generated by DNaseI on a positioned nucleosome is disrupted. Some DNA sites become hypersensitive, and some become less accessible to DnaseI.

(b) A nucleosomal species is generated that has the size of a dinucleosome and has a disrupted DNaseI cleavage pattern.

(c) The histones are transferred between two DNA molecules

(d) nucleosomes are translated
(e) randomly ordered nucleosomes are orderly spaced

(f) cruciform DNA generation

(g) alteration of the access of restriction enzymes

(h) Treatment of a closed circular nucleosomal array with Topoisomerase I followed by deproteinization gives one negative supercoil per nucleosome. A remodeler can reduce this number of supercoils without loss of the histone octamers.

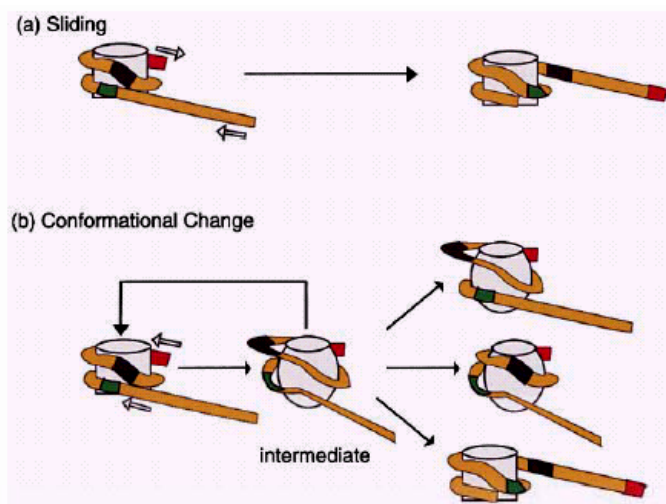


Figure 3. Two Models for the Mechanism of ATP-Dependent Nucleosome Remodeling

The structures are depicted for the intermediate, and products in (B) are hypothetical and could involve changes in the conformation of DNA, histones, or both.

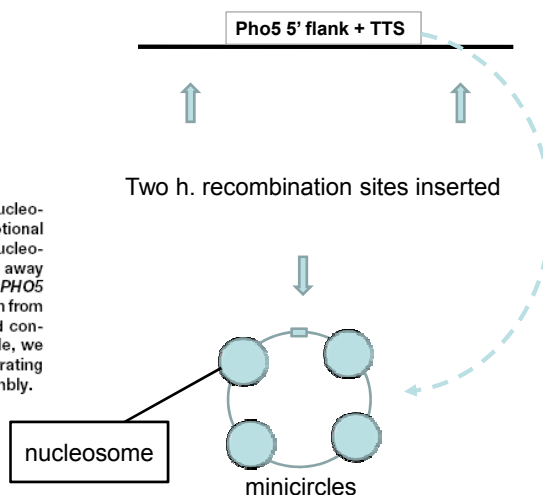
Molecular Cell, Vol. 14, 667-673, June 4, 2004, Copyright ©2004 by Cell Press

Removal of Promoter Nucleosomes by Disassembly Rather Than Sliding In Vivo

Hinrich Boeger, Joachim Griesenbeck,
J. Seth Strattan, and Roger D. Kornberg*
Department of Structural Biology
Stanford University School of Medicine
Stanford, California 94305

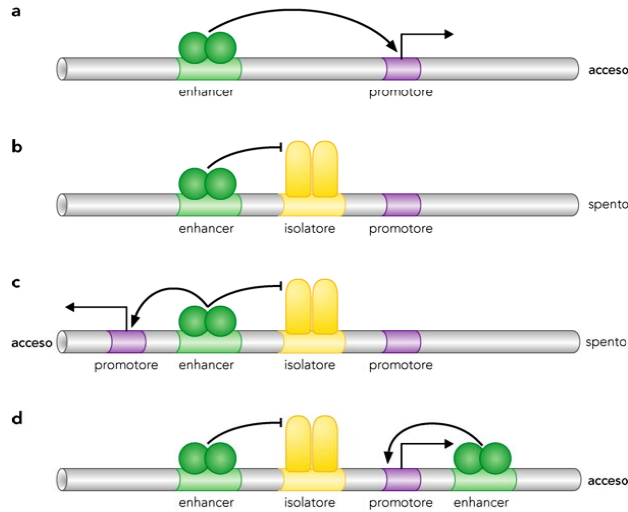
Summary

Previous work demonstrated the removal of nucleosomes from the *PHO5* promoter upon transcriptional activation in yeast. Removal could occur by nucleosome disassembly or by sliding of nucleosomes away from the promoter. We have now activated the *PHO5* promoter on chromatin circles following excision from the chromosomal locus. Whereas sliding would conserve the number of nucleosomes on the circle, we found that the number was diminished, demonstrating chromatin remodeling by nucleosome disassembly.



Gli enhancers sono sequenze regolatrici composte di molteplici siti di legame per fattori trascrizionali, localizzati in punti molto variabili del gene, anche a distanze considerevoli (50-100 Kb).

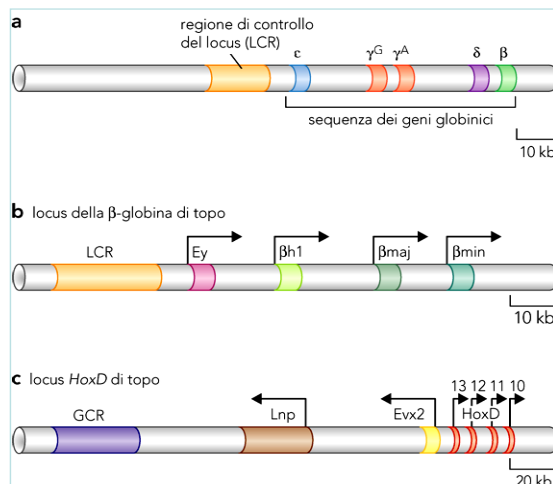
Perchè un enhancer non regola qualsiasi gene nelle vicinanze?



Particolari sequenze, chiamate isolatori (*insulators*), limitano l'effetto di un enhancer

Gruppi genici (clusters) derivati da duplicazione sono spesso regolati da una sequenza enhancer di controllo collettivo, che viene definita LCR (*locus control region*).

Gli LCR controllano l'utilizzo sequenziale ed esclusivo dei promotori dei geni del gruppo. Come esempi, il gruppo di geni che codificano le globine embrionali, fetali ed adulte; i gruppi di geni che codificano omeoproteine, espressi secondo un preciso ordine spazio-temporale.



Transcription factors mediate long-range enhancer–promoter interactions

Illias K. Nolis^{a,1}, Daniel J. McKay^{b,1}, Eva Mantouvalou^a, Stavros Lomvardas^{c,2}, Menle Merika^a, and Dimitris Thanos^{a,3}

^aInstitute of Molecular Biology, Genetics and Biotechnology, Biomedical Research Foundation, Academy of Athens, 4 Soranou Efessiou Street, Athens 11527 Greece; and ^bIntegrated Program in Cellular, Molecular and Biophysical Studies and ^cDepartment of Biochemistry and Molecular Biophysics, Columbia University, New York, NY 10032

Edited by Tom Maniatis, Harvard University, Cambridge, MA, and approved October 9, 2009 (received for review March 5, 2009)

We examined how remote enhancers establish physical communication with target promoters to activate gene transcription in response to environmental signals. Although the natural IFN- β enhancer is located immediately upstream of the core promoter, it also can function as a classical enhancer element conferring virus infection-dependent activation of heterologous promoters, even when it is placed several kilobases away from these promoters. We demonstrated that the remote IFN- β enhancer “loops out” the intervening DNA to reach the target promoter. These chromatin loops depend on sequence-specific transcription factors bound to the enhancer and the promoter and thus can explain the specificity observed in enhancer–promoter interactions, especially in complex genetic loci. Transcription factor binding sites scattered between an enhancer and a promoter can work as decoys trapping the enhancer in nonproductive loops, thus resembling insulator elements. Finally, replacement of the transcription factor binding sites involved in DNA looping with those of a heterologous prokaryotic protein, the λ repressor, which is capable of loop formation, rescues enhancer function from a distance by re-establishing enhancer–promoter loop formation.

20222–20227 | PNAS | December 1, 2009 | vol. 106 | no. 48

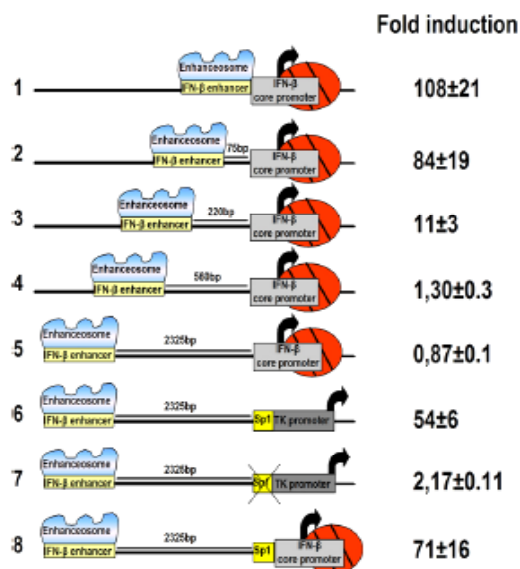
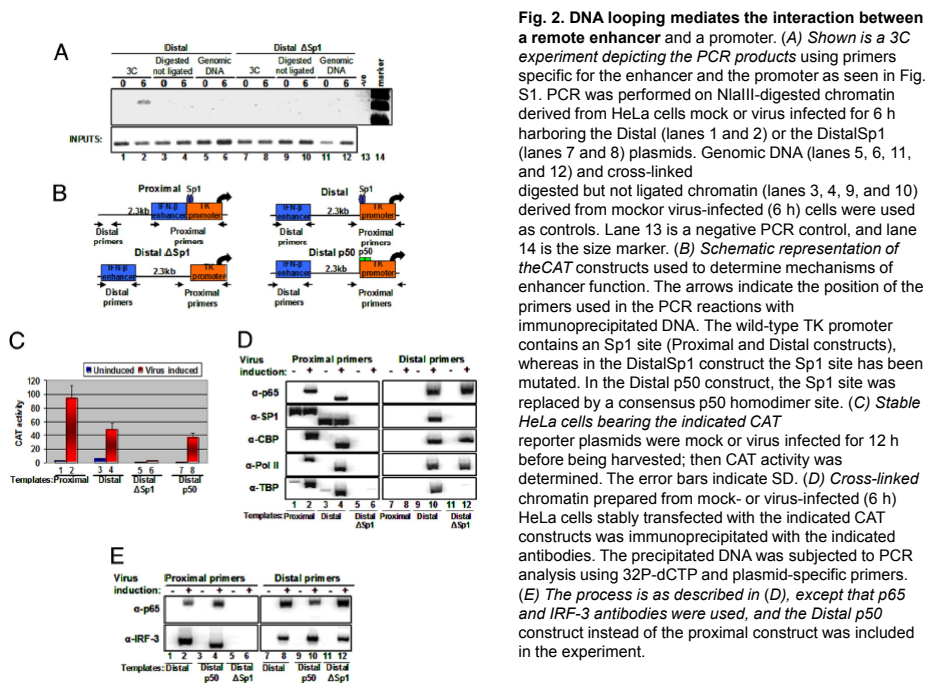
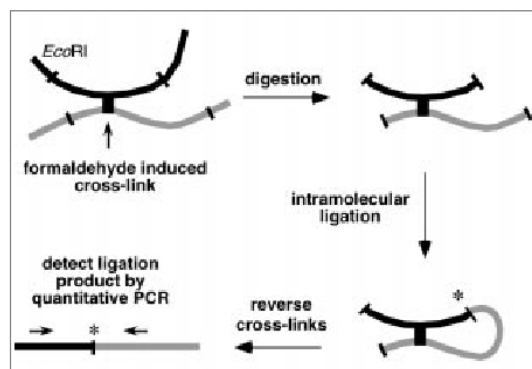


Fig. 1. Enhancer action from a distance requires upstream promoter elements. HeLa cells were transfected with the indicated chloramphenicol acetyl transferase (CAT) reporter plasmids. The cells were mock or virus infected for 24 h before being harvested. Then CAT activity was determined.



3C assay = chromosome conformation capture



Looping and Interaction between Hypersensitive Sites in the Active β -globin Locus

Bas Tolhuis,² Robert-Jan Palstra,² Erik Splinter,
Frank Grosveld, and Wouter de Laat¹
Department of Cell Biology and Genetics
Faculty of Medicine
Erasmus University, Rotterdam
P.O. Box 1738
3000DR Rotterdam
The Netherlands

Summary

Eukaryotic transcription can be regulated over tens or even hundreds of kilobases. We show that such long-range gene regulation in vivo involves spatial interactions between transcriptional elements, with intervening chromatin looping out. The spatial organization of a 200 kb region spanning the murine β -globin locus was analyzed in expressing erythroid and nonexpressing brain tissue. In brain, the globin cluster adopts a seemingly linear conformation. In erythroid cells the hypersensitive sites of the locus control region (LCR) located 40-60 kb away from the active genes, come in close spatial proximity with these genes. The intervening chromatin with inactive globin genes loops out. Moreover, two distant hypersensitive regions participate in these interactions. We propose that clustering of regulatory elements is key to creating and maintaining active chromatin domains and regulating transcription

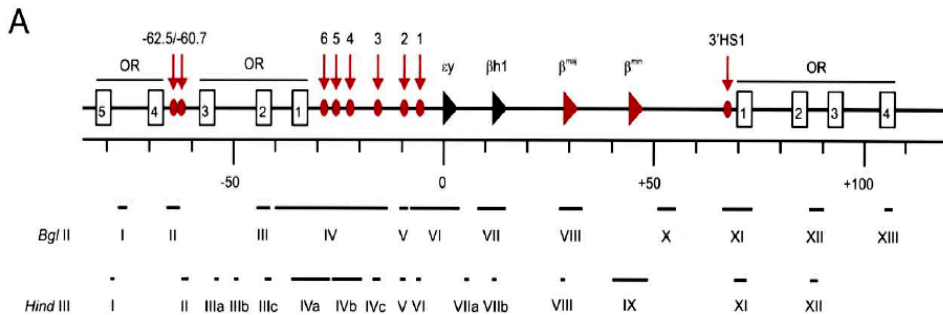


Figure 1. 3C Technology in the Murine beta-globin Locus

(A) Schematic presentation of the murine **beta-globin** locus. Red arrows and ellipses depict the individual HS. The globin genes are indicated by triangles, with **active genes (maj and min)** in red and **inactive genes (y and h1)** in black. The white boxes indicate the olfactory receptor (OR) genes (5OR1-5 and 3OR1-4). The two sets of restriction fragments (BglIII and HindIII) that were used for 3C analysis are shown below the locus. The individual fragments are indicated by Roman numerals. Identical numbering between BglIII and HindIII indicates that two fragments colocalize. Distances are in kb counting from the site of initiation of the γ gene.

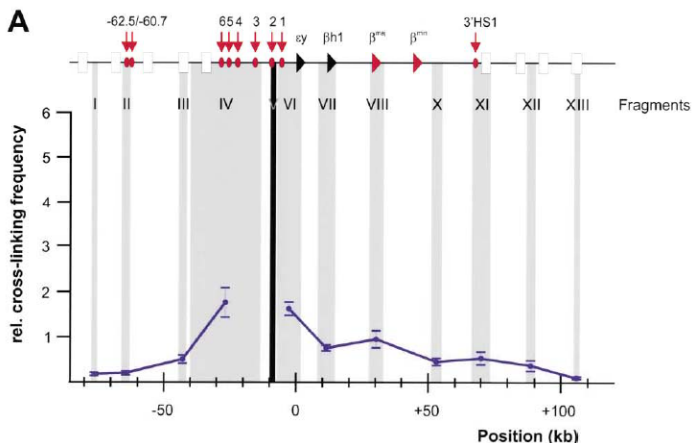
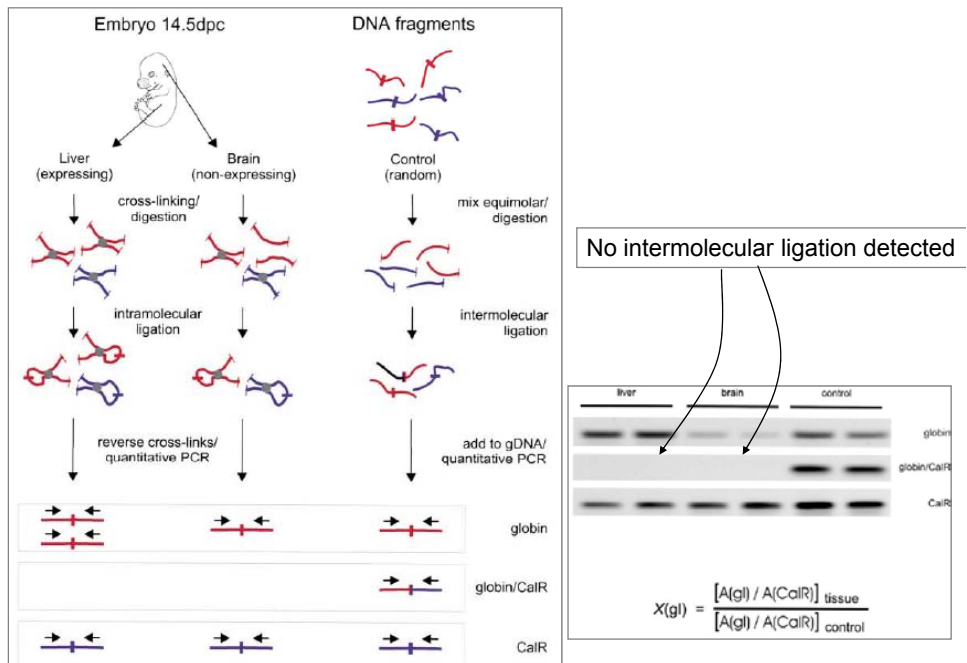


Figure 2. Linear Conformation of the beta-globin Locus in **Nonexpressing Brain Cells**. The murine γ -globin locus is depicted on top of each graph (for explanation of symbols, see Figure 1A). The x axis shows the position in the locus. The black shading shows the position and size of the fixed fragment. The gray shading indicates the position and size of other fragments. Standard error of the mean is indicated. Crosslinking frequency with a value of 1 arbitrarily corresponds to the crosslinking frequency between two neighboring CalR control fragments (with restriction sites analyzed being 1.5 kb apart). Scaling on the y axis (from 0 to 6) allows direct comparison with Figures 3–6. (A) Relative crosslinking frequencies between fixed BgIII fragment V (5HS2 in LCR) and the rest of the locus.

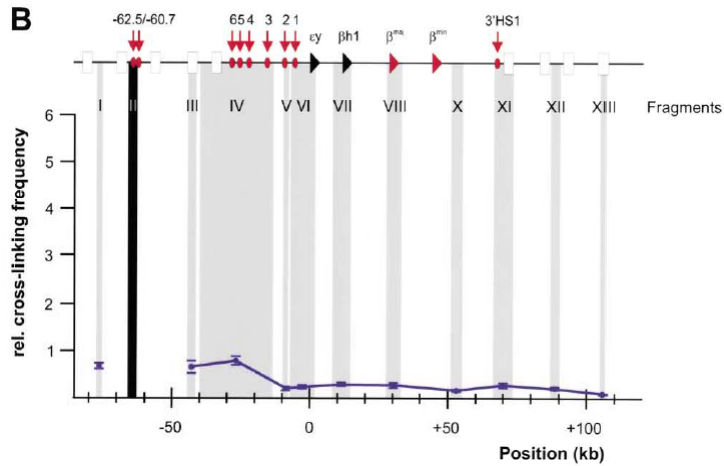


Figure 2 (B) Relative crosslinking frequencies between fixed BglII fragment II (5HS62.5/60.7) and the rest of the locus.

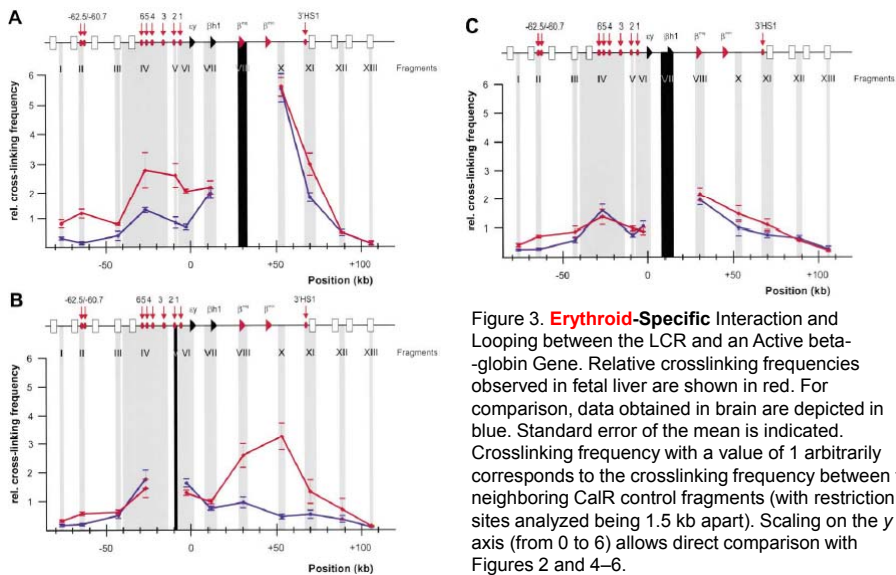


Figure 3. **Erythroid-Specific** Interaction and Looping between the LCR and an Active beta-globin Gene. Relative crosslinking frequencies observed in fetal liver are shown in red. For comparison, data obtained in brain are depicted in blue. Standard error of the mean is indicated. Crosslinking frequency with a value of 1 arbitrarily corresponds to the crosslinking frequency between two neighboring CaIR control fragments (with restriction sites analyzed being 1.5 kb apart). Scaling on the y axis (from 0 to 6) allows direct comparison with Figures 2 and 4–6.

(A) Fixed BglII fragment VIII (maj) versus the rest of the locus. (B) Fixed BglII fragment V (5HS2) versus the rest of the locus. (C) Fixed BglII fragment VII (h1) versus the rest of the locus.

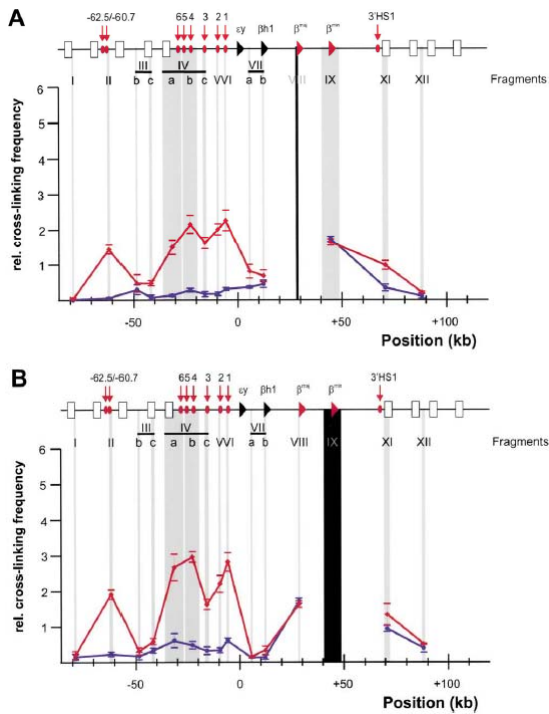


Figure 4. **Erythroid**-Specific Interactions between the Active beta-globin Genes and Individual Hypersensitive Sites in the LCR. Relative crosslinking frequencies observed in fetal liver (red) and brain (blue) are shown. Standard error of the mean is indicated. Crosslinking frequency with a value of 1 arbitrarily corresponds to the crosslinking frequency between two neighboring CalR control fragments (with restriction sites analyzed being 1.5 kb apart). Scaling on the y axis (from 0 to 6) allows direct comparison with other figures.

(A) Fixed HindIII fragment VIII Bmaj versus the rest of the locus.

(B) Fixed HindIII fragment IX (Bmin) versus the rest of the locus.

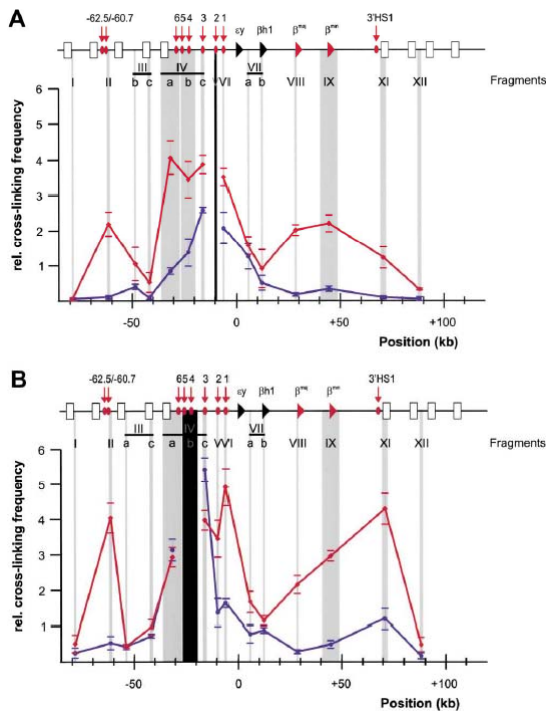


Figure 5. **Erythroid**-Specific High Crosslinking Frequencies among the Individual Hypersensitive Sites of the LCR and Two Distal Hypersensitive Sites

Relative crosslinking frequencies observed in fetal liver (red) and brain (blue) are shown. Standard error of the mean is indicated. Crosslinking frequency with a value of 1 arbitrarily corresponds to the crosslinking frequency between two neighboring CalR control fragments (with restriction sites analyzed being 1.5 kb apart). Scaling on the y axis (from 0 to 6) allows direct comparison with other figures.

(A) Fixed HindIII fragment V (5'-HS2 of the LCR) versus the rest of the locus.

(B) Fixed HindIII fragment IV-b (5'-HS4-5 of the LCR) versus the rest of the locus.

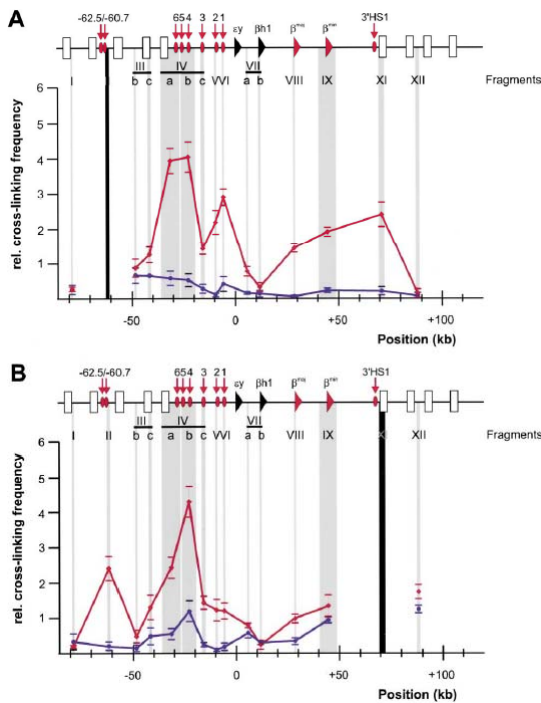


Figure 6. Two Distal Hyper-sensitive Sites at Each Side of the Locus Cluster with the LCR and the Genes. Relative crosslinking frequencies observed in fetal liver (red) and brain (blue) are shown. Standard error of the mean is indicated. Crosslinking frequency with a value of 1 arbitrarily corresponds to the crosslinking frequency between two neighboring CalR control fragments (with restriction sites analyzed being 1.5 kb apart). Scaling on the y axis (from 0 to 6) allows direct comparison with other figures. (A) Fixed HindIII fragment II (5HS62.5/60.7) versus the rest of the locus. (B) Fixed HindIII fragment XI (3HS1) versus the rest of the locus.

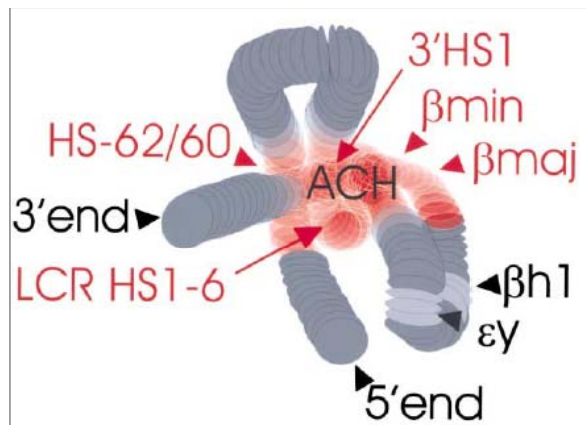


Figure 7. A 3D Model of the ACH. A hypothetical model of the active chromatin hub (ACH) is shown to illustrate the 3D nature of the ACH (not to scale), not the actual position of the elements relative to each other in vivo. Red indicates the active regions (hypersensitive sites and active genes) of the locus forming a hub of hyperaccessible chromatin (ACH). The inactive regions of the locus, having a more compact chromatin structure, are indicated in gray, with the inactive $\beta h1$ and $\epsilon\gamma$ genes in lighter gray. The olfactory genes are not shown. The interactions in the ACH would be dynamic in nature, in particular with the active genes (βmaj and βmin), which are alternately transcribed.

Interchromosomal Interactions and Olfactory Receptor Choice

Stavros Lomvardas,¹ Gilad Barnea,¹ David J. Pisapia,¹ Monica Mendelsohn,¹ Jennifer Kirkland,¹ and Richard Axel^{1,*}

¹Department of Biochemistry and Molecular Biophysics and Howard Hughes Medical Institute, College of Physicians and Surgeons, Columbia University, New York, NY 10032, USA

*Contact: ra27@columbia.edu

DOI 10.1016/j.cell.2006.06.035

SUMMARY

The expression of a single odorant receptor (OR) gene from a large gene family in individual sensory neurons is an essential feature of the organization and function of the olfactory system. We have used chromosome conformation capture to demonstrate the specific association of an enhancer element, *H*, on chromosome 14 with multiple OR gene promoters on different chromosomes. DNA and RNA fluorescence in situ hybridization (FISH) experiments allow us to visualize the colocalization of the *H* enhancer with the single OR allele that is transcribed in a sensory neuron. In transgenic mice bearing additional *H* elements, sensory neurons that express OR pseudogenes also express a second functional receptor. These data suggest a model of receptor choice in which a single *trans*-acting enhancer element may allow the stochastic activation of only one OR allele in an olfactory sensory neuron.

ARTICLE

Cell 126, 403–413, July 28, 2006 ©2006 Elsevier Inc. 403

Enhancing nuclear receptor-induced transcription requires nuclear motor and LSD1-dependent gene networking in interchromatin granules

Qidong Hu^{a,1}, Young-Soo Kwon^{b,1}, Esperanza Nunez^{a,c,1}, Maria Dafne Cardamone^{a,d}, Kasey R. Hutt^{a,e}, Kenneth A. Ohgi^g, Ivan Garcia-Bassets^g, David W. Rose^f, Christopher K. Glass^h, Michael G. Rosenfeld^{a,2}, and Xiang-Dong Fu^{b,2}

^aDepartment of Medicine, Howard Hughes Medical Institute, ^bDepartment of Cellular and Molecular Medicine, ^cBiomedical Sciences Graduate Program, ^dBioinformatics Graduate Program, ^eDepartment of Medicine, Division of Endocrinology and Metabolism, University of California at San Diego School of Medicine, La Jolla, CA 92093; and ^fDepartment of Oncological Sciences, University of Turin, 10060 Turin, Italy

Contributed by Michael G. Rosenfeld, October 22, 2008 (sent for review October 11, 2008)

Although the role of liganded nuclear receptors in mediating coactivator/corepressor exchange is well-established, little is known about the potential regulation of chromosomal organization in the 3-dimensional space of the nucleus in achieving integrated transcriptional responses to diverse signaling events. Here, we report that ligand induces rapid interchromosomal interactions among specific subsets of estrogen receptor α -bound transcription units, with a dramatic reorganization of nuclear territories, which depends on the actions of nuclear actin/myosin-I machinery and dynein light chain 1. The histone lysine demethylase, LSD1, is required for these ligand-induced interactive loci to associate with distinct interchromatin granules, long thought to serve as "storage" sites for the splicing machinery, some critical transcription elongation factors, and various chromatin remodeling complexes. We demonstrate that this 2-step nuclear rearrangement is essential for achieving enhanced, coordinated transcription of nuclear receptor target genes.

